ALMA Memo 466

Gain Stability: Requirements and Design Considerations

Larry R. D'Addario

2003-May-22

I. Background

The system temperature T_s at the inputs of the ALMA front ends is expected to range from about 50 K (band 1, SSB) to about 1000 K (band 10, DSB), depending on frequency, atmospheric conditions, and pointing elevation. Since the nominal signal level at each digitize is $P_o = 1$ mW in bandwidth $B = 2$ GHz, a net gain of $kT_sB/P_o = 75.6$ dB to 88.6 dB is required. Various losses will be incurred on the signal path, including 9 dB of power division (in Downconverter), 5 to 20 dB in variable attenuator headroom, about 6 dB in padding (for matching), 7 dB in second mixer conversion loss, estimated 11 dB in insertion loss of various components, and estimated 8 dB in cables and connectors. The required active gain is then 122 to 150 dB. Since most of the active gain is fixed and independent of band, and in order to allow for worst-case component tolerances and the possibility of additional padding, the actual active gain will be larger than 150 dB.

In order to support total power radiometry, it has been suggested that the net gain must be very stable. There is no actual specification on this. The ALMA Project Book [1] mentions only a 1% limit in connection with calibration accuracy, but a limit on the fractional power gain fluctuation of $\delta G/G = 1 \times 10^{-4}$ has been proposed in recent discussions. This follows from a desire that the sensitivity not be limited by the instrumental gain fluctuations, but rather by thermal noise or by fluctuations in atmospheric emission. In [2], it is argued that the most stringent requirement occurs for on-the-fly total power scanning with 8 GHz bandwidth, and that for this case the 1×10^{-4} value applies at intervals of 1 sec in order that the gain fluctuation noise not exceed the thermal noise. In [3], it is argued that this mode will incur errors due to fluctuation of atmospheric emission of about .015 K at 230 GHz at the 50th percentile; this has the same effect as $\delta G/G = 1 \times 10^{-4}$ if $T_s = 150$ K. Documents giving a formal requirement for ALMA are in preparation [4][5].

At other time scales, different requirements may prevail. For beam-switched total power continuum (using subreflector nutation), fractional gain stability as small as 1.3×10^{-5} might be needed in order not to limit sensitivity, but only for time intervals of .05 sec (assuming 10 Hz switching with 20% transition time). For interferometry, the gain should be stable over a gain calibration cycle, which may be several seconds to several minutes [4], but the fractional variation can be several$\times 10^{-3}$ since the calibration error is unlikely to be less than 1×10^{-2}.

Fractional gain stability better than 1×10^{-3} is very difficult on any of these time scales, especially since the large total gain must be implemented in many separate stages. With K identical stages having independent gain fluctuations, each must have a fractional stability $1/\sqrt{K}$ times the total. In practice, the stages are not at all identical, so some must be much better than this. Also, gain variations caused by the environment are unlikely to be independent among stages; for identical but fully correlated fluctuations, the fractional stability of each stage must be $1/K$ times the total.

In ALMA, the active components of the signal processing chain may be classified as follows.

- Cold RF amplifier (bands 1 and 2 only);
- SIS mixer (bands 3–9) or cold Schottky diode mixer (bands 1 and 2);
- Cold IF amplifier, 4–12 GHz;
- Room temperature IF amplifier(s), 4–12 GHz;
- Room temperature baseband amplifier(s), 2–4 GHz.

We will assume that passive components (filters, switches, power dividers, etc.) have negligible gain variation on the time scales of interest, and we also neglect any gain variation of the second mixer. The different types of active components each contribute differently to the gain variation, and different ones may be dominant on different time scales. Furthermore, we distinguish two causes of gain variation for each device: "intrinsic" fluctuations, caused by physical mechanisms internal to the device, such as charge density fluctuations in semiconductors, which are truely random processes characterized by well behaved statistics and which are independent from one device to another; and "extrinsic" fluctuations, caused by changes in the environment

(primarily temperature, but possibly pressure and mechanical stress) or in auxillary signals like d.c. bias or LO power. The causes of extrinsic fluctuations may be deterministic or even periodic, or their statistics may be less well behaved.

II. Theory

Radiometer Output Noise

Consider the simplified model of a radiometer illustrated in Figure 1. The input $n(t)$ is white gaussian noise at constant noise temperature T_s, and it includes both the radiometer's noise and any external signal ("sky") noise. This system observes an input band centered at f_0 with effective bandwidth B, determined by an ideal bandpass filter. We assume for simplicty that $B << f_0$. The net voltage gain is $g(t) = g_0 + \delta g(t)$. The detector is taken to be an ideal square-law device. It is followed by a low pass filter with bandwidth $> B$ that rejects only the RF components near $2f_0$. (To make a practical radiometer, an integrate-and-dump filter should be added to the output of this model.)

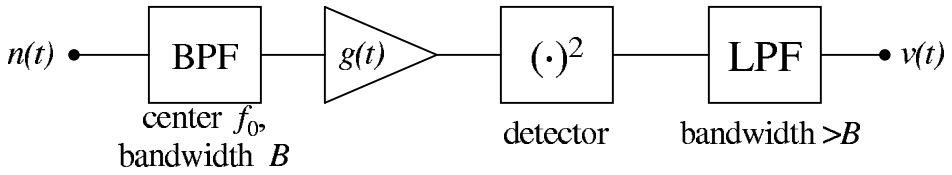

Figure 1: Simple radiometer model.

Any simple radiometer, including but not limited to the model of Fig. 1, can be experimentally characterized by measuring the power spectral density of the wideband ("video") output of its square law detector. In the absence of gain fluctuations, this spectrum should be nearly flat at $(V_0/B)^2$ for frequencies $<< B$, where V_0 is the average value of the detector output. In practical measurements, e.g. [6], this is indeed observed at high frequencies, but at low frequencies (typically below 5 to 1000 Hz) the spectral density often increases in proportion to f^α, where $\alpha \approx -1$. The excess spectral density is usually attributed to gain fluctuations.

As shown in Appendix A, the relative power spectral density of the output voltage $v(t)$ in the model of Fig. 1 is given by

$$\frac{S_v(f)}{V_0^2} = \delta(f) + \frac{1}{B} + \frac{2S_g(f)}{G_0}, \quad |f| << B \tag{1}$$

where $V_0 = \langle v(t) \rangle$ is the average (d.c.) output, $G_0 = |g_0|^2$ is the average power gain, and $S_g(f)$ is the power spectral density of $\delta g(t)$, so that it is the Fourier transform of

$$R_g(\tau) = \langle \delta g(t)\, \delta g(t-\tau) \rangle. \tag{2}$$

Therefore, if the gain fluctuations are such that $S_g(f) = G_1(f/f_1)^\alpha$, then we expect the spectral density to have the form that is often observed. These gain fluctuations are then described by parameters G_1, f_1, and α, or alternatively by B, α, and "corner frequency" $f_c = f_1(BG_1)^{-1/\alpha}$, which is the frequency at which the last two terms in (1) are equal. On the other hand, $S_g(f)$ cannot maintain this power law form with $\alpha < 0$ down to $f = 0$, because $R_g(0) = \langle \delta g(t)^2 \rangle$ would then be infinite.

At sufficiently low frequencies, gain fluctuations in most active devices are assumed to be dominated by variations in the environment. At sufficiently high frequencies, the gain fluctuations are usually negligible compared with the detector output fluctuations due to the noisy nature of the input (which is partly the thermal noise of the radiometer itself). At other frequencies, experiments show that the fluctuations have a negative power law spectrum. For some devices, especially HFET amplifiers, this is roughly consistent with the effect of expected fluctuations in charge carrier density in the active regions of transistors, but a detailed theory is currently lacking.

Application to Radio Telescopes

A single radiometer measurement involves averaging the output voltage for integrating time T_i. All astronomical measurements then consist of differences between such radiometer measurements, where a reference observation is subtracted from a signal or "on source" observation. The signal-reference cycle is usually repeated, and the differences are further averaged to achieve greater SNR. The period of the switching cycle is $2T \geq T_{is} + T_{ir}$, where T_{is} and T_{ir} are the signal and reference integrating times, respectively. Thus, the result of one astronomical measurement is

$$\Delta V = \frac{1}{T_{is}} \int_0^{T_{is}} v(t)\, dt - \frac{1}{T_{ir}} \int_{T_1}^{T_1+T_{ir}} v(t)\, dt. \tag{3}$$

The measurement accuracy is characterized by the variance of ΔV, and this depends on the system noise temperature, the bandwidth, the integrating times, and the gain fluctuations. Whereas the astronomical signal that gives rise to ΔV is usually a small fraction of the input signal, the variance will be the same if $\langle \Delta V \rangle = 0$, so we calculate it for that case. Then

$$\operatorname{var} \Delta V = \langle \Delta V^2 \rangle - \langle \Delta V \rangle^2 = \langle \Delta V^2 \rangle \tag{4}$$

and taking for simplicity $T_{is} = T_{ir} = aT$, $a \leq 1$, and $T_1 = T$, substituting (3) into (4) gives

$$\operatorname{var} \Delta V = 2 \frac{1}{a^2 t^2} \left[\int_0^{at} \int_0^{at} R_v(t - t')\, dt\, dt' - \int_0^{at} \int_T^{T+at} R_v(t - t')\, dt\, dt' \right] \tag{5}$$

where $R_v(\tau)$ is the autocorrelation function of $v(t)$ and hence the Fourier transform of $S_v(f)$. Using the latter fact and carrying out the time integrals produces

$$\operatorname{var} \Delta V = \frac{1}{a^2 t^2} \int_{-\infty}^{\infty} S_v(f) \frac{(1 - \cos 2\pi f T)(1 - \cos 2\pi f a T)}{\pi^2 f^2}\, df. \tag{6}$$

One can now substitute $S_v(f)$ from (1) and carry out the frequency integral to obtain the variances for cases of interest.

$\operatorname{var} \Delta V$ is sometimes called the "Allan variance" of the radiometer output [7][8]. Indeed, $\operatorname{var} \Delta V / V_0^2$ is identical to the two-sample Allan variance $\sigma^2(2, T, aT)$ [9] used to characterize the stability of oscillators if $v(t)/V_0$ is used in place of the fractional frequency variation $f(t)/f_0$ of the oscillator. We can therefore use the well-developed theory of oscillator stability to understand the relationships among measurable quantities. For example, if $S_v(f) = h_{-2}/f^2$ for constant h_{-2}, as is sometimes observed when gain fluctuations dominate, then $\sigma(2, T, T) = (4\pi^2/3) h_{-2} |T|$ and this $v(t)$ may be described as a random walk [10]. Actually, most data (see section III below) show $S_v(f) = h_\alpha f^\alpha$ with $\alpha \approx -1$. When $\alpha = -1$, it is found that $\sigma^2(2, T, T) = 4 \ln 2\, h_{-1}$ and the fluctuations are described as "flicker." This is the statistical behavior that is called "$1/f$ noise" in the context of oscillator stability. Finally, when the spectral density is constant, $S_v(f) = 1/B$, as it is when the thermal noise at the radiometer's input is dominant [see (1)], it is found that $\sigma^2(2, T, T) = 1/(BT)$, in agreement with the usual radiometer equation.[1] These relationships are illustrated in Figure 2. (When $a < 1$, which implies non-zero blanking time between signal and reference, the appropriate formulas are given in [10].)

[1] The formulas for σ^2 given here are 2 times larger than those in [10] because that paper used single-sided spectral densities while we have defined $S_v(f)$ to be two-sided.

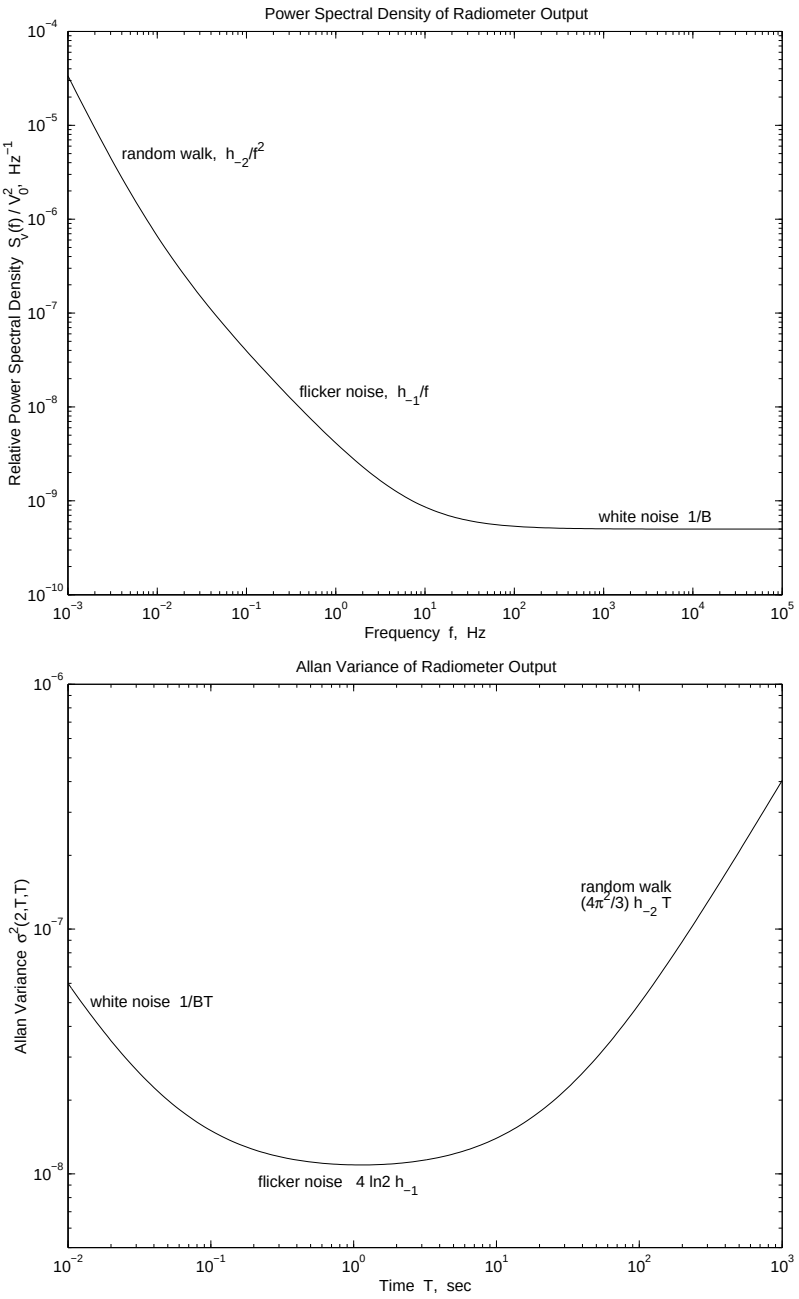

Figure 2: Frequency domain (top) and time domain (bottom) representations of radiometer output noise. Parameters have been choosen so that the dominant noise is from random-walk gain fluctuations at low frequencies and long times, flicker gain fluctuations at intermediate frequencies and times, and thermal noise at high frequencies and short times.

III. Experimental Data on Intrinsic Gain Fluctuations

In this section, available data on intrinsic gain fluctuations is reviewed, concentrating on devices relevant to the ALMA signal processing chain, as identified in section I.

For SIS mixers, little is known about intrinsic gain fluctuations. There is some sparce data on the gain stability of complete SIS receivers [7][11], and it is consistent with intrinsic gain variations of the cryogenically cooled stages of IF amplification and with extrinsic causes of mixer gain variation (see section IV below).

No available theory suggests a mechanism for intrinsic mixer gain fluctuations, but neither are they ruled out.

For microwave amplifiers, including those at RF, IF and baseband, considerably more is known, but our knowledge is far from complete. In HFET devices, known physical mechanisms are believed to cause random fluctuations in the number of available charge carriers and in their mobility, leading to fluctuations in gain that should have flicker statistics [14]. The gain variance should be inversely proportional to the active area of the device (gate length times width) and to the drain current. There are some indications that InP devices have larger gain fluctuations than GaAs devices [13]. Cooling to cryogenic temperatures leads to larger gain fluctuations, although this is partly due to the use of lower drain current for lower noise temperature. Wollack [14] reports maximum fluctuations at 150K in GaAs devices, but Wollack and Pospieszalski [6] find a linear decrease with temperature from 60 to 300K in InP devices. In GaAs devices, illumination with an LED at cryogenic temperatures causes increased fluctuations [14]. There also seems to be considerable variation among devices that are nominally identical, especially if they are from different wafers.

Table 1: Reported gain fluctuation parameters for radiometers

Ref	*Type*	*T1* K	*N1*	*A1* μm^2	*T2* K	*N2*	*A2* μm^2	f_0 GHz	*B* Hz	*fknee* Hz	α	G_1 Hz^{-1}	*per stg* Hz^{-1}	$G_{1,norm}$ $\mu m^2 Hz^{-1}$	*Notes*
[11]	InP	40	1	5	40	4	10	41.6	6.90E+09	64	-0.84	4.77E-09	9.54E-10	1.69E-09	Q1 TOCO
[11]	InP	40	1	5	40	4	10	41.4	7.30E+09	168	-1.57	4.27E-07	8.54E-08	1.51E-07	Q2 TOCO
[11]	InP	40	1	5	40	4	10	42.1	5.30E+09	37	-0.84	3.92E-09	7.84E-10	1.38E-09	Q3 TOCO
[11]	InP	40	1	5	40	4	10	41.7	4.50E+09	42	-0.88	5.96E-09	1.19E-09	2.11E-09	Q4 TOCO
[11]	InP	2.7	1	5	2.7	4	10	41.3	7.50E+09	686	-0.82	2.82E-08	5.65E-09	9.28E-09	Q2 QMAP
[11]	InP	2.7	1	5	2.7	4	10	42.1	6.30E+09	20	-0.78	1.64E-09	3.28E-10	5.40E-10	Q3 QMAP
[11]	InP	2.7	1	5	2.7	4	10	41.2	7.00E+09	67	-0.71	2.83E-09	5.66E-10	9.30E-10	Q4 QMAP
[25]	GaAs	15	4	25	1	0	1	30.0	3.00E+09	2	-1.00	6.67E-10	1.67E-10	8.84E-10	
[6]	InP	54	10	5	1	0	1	82.0	3.00E+09	1500	-0.90	2.41E-07	2.41E-08	2.55E-08	
[6]	InP	54	10	5	1	0	1	82.0	2.00E+10	8000	-0.90	1.63E-07	1.63E-08	1.73E-08	
[13]	InP	14	1	15	14	1	50	8.0	n/a	n/a	-1.16	1.00E-08	5.00E-09	2.40E-08	
[13]	InP	14	1	40	14	1	50	8.0	n/a	n/a	-1.02	6.08E-09	3.04E-09	2.77E-08	
[13]	InP	14	2	50	1	0	1	8.0	n/a	n/a	-1.40	2.30E-09	1.15E-09	1.22E-08	
[14]	GaAs	18	4	25	1	0	1	30.0	2.70E+09		-0.90	2.40E-09	6.00E-10	3.18E-09	
[14]	GaAs	18	4	25	1	0	1	30.0	2.70E+09		-0.90	3.60E-09	9.00E-10	4.77E-09	
[14]	GaAs	18	5	10	1	0	1	45.0	4.40E+09		-0.90	8.20E-09	1.64E-09	3.48E-09	
[14]	GaAs	18	5	10	1	0	1	45.0	3.80E+09		-0.90	7.10E-09	1.42E-09	3.01E-09	
[14]	GaAs	18	5	10	1	0	1	45.0	5.00E+09		-0.90	5.40E-09	1.08E-09	2.29E-09	
[6]	InP	300	10	5	1	0	1	82.0	2.00E+10	850	-0.90	2.16E-08	2.16E-09	2.30E-09	
[13]	InP/Ga	300	1	40	300	1	50	8.0	n/a	n/a	-1.02	7.84E-10	3.92E-10	5.69E-09	
[13]	InP/Ga	300	1	40	300	1	50	8.0	n/a	n/a	-1.32	3.24E-10	1.62E-10	2.35E-09	
[13]	GaAs	300	2	50	1	0	1	8.0	n/a	n/a	-1.00	7.84E-10	3.92E-10	4.16E-09	

Note: In some cases, not all amplifier stages are identical. The table allows for $N1$ stages at temperature $T1$ with area $A1$ (gate length×width), and $N2$ stages at $T2$ and $A2$. Measurements were made at center frequency f_0 and bandwidth B. Other column headings are defined in the text.

Table 1 summarizes experimental data on HFET amplifiers from the literature. The data are taken from five papers [6][11][13][14][25], and they include amplifiers with GaAs and InP transistors of several sizes, center frequencies from 8 GHz to 82 GHz, and physical temperatures from 2.7 K to 300 K. In each case, the measurements have been reduced to estimates of the parameters G_1 and α for $f_1 = 1\,\mathrm{Hz}$. Ignoring one extreme outlier, the overall range of α is $[-1.41, -0.7]$ and of G_1 is $[3.2\times10^{-10}, 2.4\times10^{-7}]$ Hz^{-1} (743:1). After accounting for variations in the device areas, physical temperatures, and number of amplifier stages in each measurement, the range of G_1 is reduced to $[5.4\times10^{-10}, 2.8\times10^{-8}]$ $\mathrm{Hz}^{-1}\,\mu\mathrm{m}^2$ per stage at 300K (51:1). This was done by scaling according to

$$G_{1,\mathrm{norm}} = G_1[70\mathrm{K}/(300\mathrm{K} - T)]A/N, \tag{7}$$

where N is the number of stages, A is the device area, and T is the physical temperature. The temperature factor is an empirical fit to the data in [6], measured for InP devices and perhaps not appropriate to all materials. In some cases, the first amplifier stage was different from the others; then the scaling factor was a sum of separate terms, each similar to (7), for each stage. No attempt was made to scale for biasing differences, since that information is mostly not reported. Usually the bias of the first stage was set for minimum noise temperature, with other stages biased at higher drain current.

There were differences among the methods used by different authors, perhaps accounting for some of the variation in results. The measurements in [11] were for complete radiometers that included room temperature stages; our analysis assumes that the cryogenic stages are dominant and makes no correction. In [14], it is claimed that the reported results have been corrected for room temperature stages. In [6], ten stages of the device under test were used, ensuring that its fluctuations dominate. These three papers all measured the power spectrum $S_v(f)$ of the detector output with broad-band noise at the radiometer's input; they used $S_g(f) = G_1(f/f_1)^\alpha$ in equation (1) and determined G_1 and α by fitting to the measurements. In contrast, [13] used a CW test signal at the input and observed the gain fluctuation spectrum more directly.

From the normalized results, it is possible to make these observations:

- There is no apparent dependence on center frequency, with the 8 GHz results for $G_{1,\mathrm{norm}}$ covering about the same range as the 82 GHz results. However, higher frequency amplifiers generally use transistors of smaller area, and each stage has smaller gain; it is for these reasons that the fluctuations in a multi-stage amplifier of a given total gain are higher at higher frequencies.
- There is no apparent dependence on device material, with the scaled results covering about the same range for GaAs-based and InP-based devices.
- The empirical temperature scaling from [6] appears to work well, since there is no apparent temperature dependence after scaling. There is much more scatter in the measurements at cryogenic temperatures ($[5.4 \times 10^{-10}, 5.8 \times 10^{-8}]\,\mathrm{Hz}^{-1}\,\mu\mathrm{m}^{-2}$, or 51:1) than in those at room temperature ($[2.3 \times 10^{-9}, 5.7 \times 10^{-9}]\,\mathrm{Hz}^{-1}\,\mu\mathrm{m}^{-2}$, or 2.5:1). However, the room temperature data includes only a few amplifiers.

IV. Experimental Data on Extrinsic Gain Sensitivities

The gain of a typical heterodyne radiometer is subject to many influences from the environment and from auxilliary signals, including

- temperature changes, especially for active components but also for some passive ones such as filters;
- mechanical stress changes, particularly for cables and other items of extended size, especially on antennas where the relative direction of gravity is variable;
- variations in d.c. bias voltages or currents to active devices, including amplifiers and mixers;
- variations in local oscillator power supplied to mixers, especially SIS mixers and unsaturated resistive mixers (resulting mainly from temperature and bias variations in the LO source); and
- possibly, variations in the magnetic field within SIS mixers (which is known to have a strong influence on mixer noise temperature at high frequencies, but where the influence on gain appears to be unknown).

Clearly the situation is very complicated, making a comprehensive treatment difficult. Here we concentrate on reviewing what is known experimentally about the sensitivity of gain to some of these factors. We will ignore mechanical stress effects on the assumption that they can be made negligible by good structural design.

The most detailed work to date on the stability of SIS receivers is reported in [7]. (The theory and analysis in this paper are poorly developed, but it gives valuable experimental results.) Additional results are given in [15] and [16]. New studies for ALMA are underway at SRON [17] with results expected in the near future.

Data on the sensitivities of other components is very limited, but some is given in [16].

Some data on the stability of complete millimeter-wave receivers is given in [18] as Allan variance plots. Measurements are reported for each of the two channels of the 100 GHz and 230 GHz receivers on the IRAM 30 Meter Telescope. In most cases, $\mathrm{var}\,\Delta V(\tau)/V_0^2$ is dominated by flicker-type gain fluctuations for $\tau > 0.1\,\mathrm{sec}$ and by random-walk fluctuations for $\tau > 30\,\mathrm{sec}$. Typically $\mathrm{var}\,\Delta V(1\,\mathrm{sec})/V_0^2 = 2 \times 10^{-8}$, but two receivers did much better, $< 5 \times 10^{-9}$, at a particular LO frequency. It is not known how much of the variance is intrinsic and how much is extrinsic, nor how much is due to each of the many components in the signal path.

Table 2: ReportedTemperature Coefficients

Ref	*Device*	*(1/G)dG/dT* K^{-1}	*T* K	*dT* for *dG/G*= 1e-4 K	*Notes*
[15]	SIS 100 GHz	0.05	3.8	0.0020	
[7]	SIS 345 GHz	-0.1	3.8	-0.0010	1 junction
[7]	SIS 345 GHz	-0.22	4.2	-0.0005	
[7]	HFET 1.5 GHz	0.03	5	0.0033	
[15]	HFET 1.8 GHz	0.008	14	0.0125	
[15]	amps + det	-0.013	300	-0.0077	
[16]	L band amp	-0.0021	300	-0.0476	UTC27xx (NEC)
[16]	L band filter	-0.0012	300	-0.0833	~octave BW
[16]	L band mixer	-0.00035	300	-0.2857	MDC169 (Anzac)
[16]	UHF amp/filter	-0.0023	300	-0.0435	UTC27xx
[16]	sq law detector	-0.007	300	-0.0143	not due to dc offset

Temperature Coefficients

The results discussed here are summarized in Table 2.

Kooi [7] and Plambek [15] provide data on $(1/G)dG/dT$ for an SIS mixer separately from its IF amplifier and other components. Kooi used a single-junction 345 GHz mixer with fixed-voltage bias and varied the temperature from 2 to 10 K. The temperature coefficient approaches zero at 2K and is maximum at 5K. At 3.8K, he measures –0.1 K^{-1}. Meanwhile Plambeck measures $|(1/G)dG/dT| = .05\,K^{-1}$ at 3.8K for a 100 GHz mixer. It is not known whether the difference is due to mixer construction or frequency. At 4.2K, a more practical temperature in large and complex receivers, the coefficient is larger by at least a factor of 2.

For HFET amplifiers at cryogenic temperatures, Kooi measures $.03\,K^{-1}$ and Plambek measures $.008\,K^{-1}$ (signs not reported). Both of these used GaAs devices at 1–2 GHz. It is not known how much of this might be due to bias circuit components. Probably both used constant-current bias.

Plambek [19] and Frey [16] provide data for various microwave and UHF components used in the receivers at the BIMA array. These form a room temperature chain of amplifiers, filters, mixer, and detector starting at 1.3–2.2 GHz with an estimated 60 dB of active gain. In this system, the dominant component is the square law detector (type not reported), which accounts for 54% of the –.013 K^{-1} total temperature coefficient. All components of the chain have negative temperature coefficients, so there is no cancellation. For the amplifiers, 30% of the coefficient is due to the associated voltage regulator (–1 mV/K), and another 10% is due to a ceramic circuit board. With all components mounted on a plate inside an enclosure, temperature regulation of .02 K peak-to-peak in 24 hours and .01 K in 1 hour is achieved, limiting the gain variation to 1.3×10^{-4} per hour or, probably, 4×10^{-8} per second. All of these are laboratory results, and it is estimated [19] that the performance on the telescope may be 10 times worse.

Other Influences

The sensitivities of amplifiers to bias voltages and currents and of resistive mixers to LO power are reasonably well understood.

The gain of an SIS mixer is also sensitive to bias voltage and LO power, and so is its noise temperature. Such mixers are normally adjusted for minimum noise temperature, and this frequently (but not always) correspondends to a local maximum of the gain. In that case, the first-order sensitivities dG/dV_b and dG/dP_L are zero, where V_b is the bias voltage and P_L is the LO power. But adjustment to the optimum operating point is not perfect, so second-order effects are important. To obtain a rough idea of the magnitude, let $P_{\rm opt}, V_{\rm opt}$ be the optimum LO power and bias voltage, respectively, and assume that the gain goes quadratically to zero at $P_L = P_{\rm opt} \pm P_{\rm opt}$ and at $V_b = V_{\rm opt} \pm hf_L N_j/2e$, where h is Plank's constant, f_L is the LO frequency, N_j is the number of series-connected SIS juntions, and e is the electronic charge. Thus, the relative LO sensitivity is independent of frequency but the bias sensitivity gets smaller with frequency because the photon step width $hf_L N_j/e$ gets larger. Then

$$\frac{G - G_{\rm max}}{G_{\rm max}} = -\left(\frac{V_b - V_{\rm opt}}{hf_L N_j/2e}\right)^2 - \left(\frac{P_L - P_{\rm opt}}{P_{\rm opt}}\right)^2, \tag{8}$$

so an LO power error of 10% or a bias error of 5% of the photon step leads to a gain change of –1%.

V. Application To ALMA

It is expected that total power radiometry will produce the most stringent requirements for gain stability.

The ALMA receivers allow three ways of making broad-band total power measurements. Signals are converted to baseband channels of 2 GHz bandwidth, of which there are 4 per polarization. First, each of these is digitized and the samples are digitally detected at the correlator. The correlator allows integration times as small as 1.0 msec. Second, a copy of the signal driving each digitizer also drives an analog square law detector. Third, each IF signal from the front end drives a separate analog square law detector observing the full 8 GHz IF bandwidth, although the front ends for some bands provide only 4 GHz of useful bandwidth. Each analog detector has an integrate-and-dump filter with integration time as small as 2 msec. Nearly the same radiometric sensitivity is available via all three methods. Using the broad IF detectors avoids some analog signal processing and might produce better gain stability. Combining the measurements from several baseband channels is not expected to allow gain fluctuations to be averaged out, since intrinsic fluctuations are expected to be mainly in the front end (common to all baseband channels) and since extrinsic influences are expected to be well correlated among the channels. For this discussion, $B = 7\,\mathrm{GHz}$ is used throughout as a good approximation to the single-polarization effective bandwidth for all detection methods.

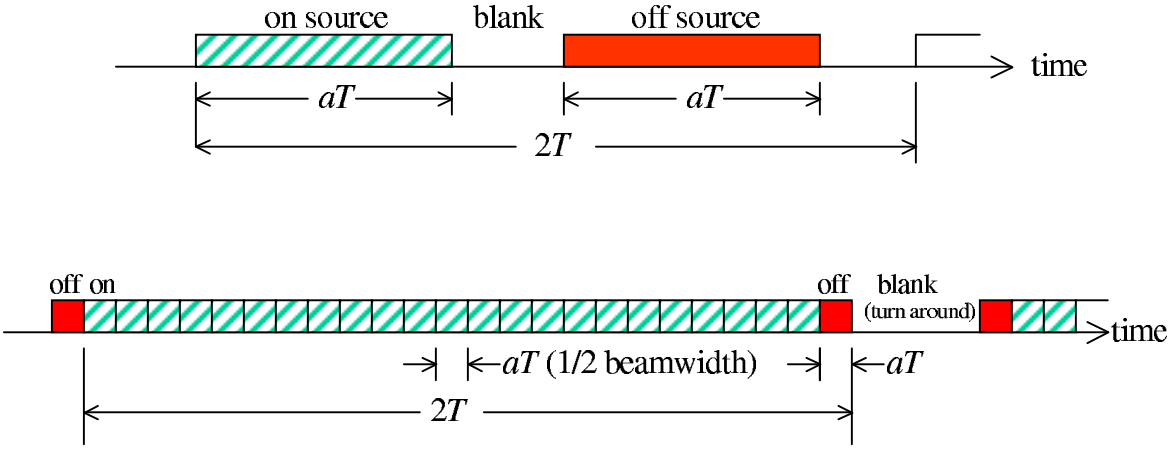

Figure 3: Observing time sequences. Top: Beam switching mode. Bottom: On-the-fly mode.

Following the arguments in [2], consider two modes for such observations: beam switching via nutation of the subreflector; and on-the-fly (OTF) mapping. Figure 3 shows plots of the time sequence for one cycle of each of these modes. In beam switching, we take the cycle time to be $2T = 0.1\,\mathrm{sec}$ with 10 msec transition time, based on the specifications for the nutation drive performance [20]. In OTF mapping, we take the on-source scan time to be fixed at 1.0 sec for any source size; at 0.5 deg/sec maximum scanning speed, this allows sources up to 0.5 deg across. The scan is broken into many integrations, and we take each to have a duration of $(1/2)\theta_b/\dot{\theta}$ where θ_b is the half-power beamwidth angle and $\dot{\theta}$ is the angular scanning speed (i.e., 2 points per beam). Dead time between integrations is assumed negligible. Off-source reference measurements are made between OTF scans while the antenna motion reverses direction. The reference measurements are subtracted from the on-source measurements, but there are several ways that this might be done. The average of the two end measurements surrounding a scan might be used as the reference for all on-source integrations, or the end measurement nearest to each might be used. Usually the off-source time is significant because the antenna acceleration is limited, so the integration time could be much longer than for each on-source sample; or the reference integration could be limited to a portion of the off-source time that is nearest to the on-source scan. The best choice depends on whether errors are dominated by thermal noise, instrumental gain fluctuations, temporal fluctuations in atmospheric transmission or emission, or spatial fluctuations in atmospheric transmission or emission. In this discussion, where we are concentrating on the effects of gain fluctuations, we assume a strategy that uses an off-source integration time equal to the on-source integration time, with the nearest off-source integration serving as reference for each on-source

integration. This is illustrated in Fig. 3. In the absence of any instrumental and atmospheric fluctuations, longer off-source integrations could reduce the variance for each on-off difference by at most a factor of 2.

Under these assumptions, $\mathrm{var}\,\Delta V/V_0^2$ for each mode can be written as the Allan variance $\sigma^2(2, T, aT)$ where

Beam switching: $T = 0.05\,\mathrm{sec}$, $aT = 0.04\,\mathrm{sec}$

OTF mapping: $T = 0.5\,\mathrm{sec}$, $aT = \theta_b/(0.5\,\mathrm{deg/sec})$

and the OTF integration time assumes the maximum source size (0.5 deg).

Table 3: Gain Fluctuations Equal To Thermal Noise

All cases: $B = 7\,\mathrm{GHz}$. OTF: $\dot\theta = 1\,\mathrm{deg/sec}$, 1 sec/scan, 2 integrations/beam.

Mode	θ_b (f_L) arcsec (GHz)	aT sec	T sec	$(BT)^{-1/2}$ [a] (thermal noise)	G_1 [b] $\mathrm{Hz}^{-1/2}$	@.013/K [c] (typ. 300K)	@.05/K [c] (typ. SIS)	$\dot G/G$ [d] sec^{-1}
Beam sw.	n/a	.04	.05	6.0×10^{-5}	1.1×10^{-9}	4.6 mK	1.2 mK	.0012
OTF	57 (90)	.017	.517	9.3×10^{-5}	1.4×10^{-9}	7.1 mK	1.9 mK	.00019
OTF	18 (270)	.0052	.505	1.6×10^{-4}	3.6×10^{-9}	12 mK	3.2 mK	.00032
OTF	5.7 (900)	.0017	.502	2.9×10^{-4}	1.0×10^{-8}	22 mK	5.8 mK	.00058

[a] This is the rms error in $\Delta V/V_0$ due to thermal noise alone.

[b] Coefficient of gain fluctuation spectrum if it is entirely of flicker-noise type (using formulas in [10]).

[c] At the given temperature coefficient, rms temperature change in interval T if gain fluctuation is entirely due to temperature.

[d] Fractional rate of change if gain variation is due to steady drift.

Table 3 shows the standard deviation of $\Delta V/V_0$ that results from thermal noise, $1/\sqrt{BT}$. If this is the same as the rms gain change in interval T, then the total rms error is $\sqrt{2}$ larger than with thermal noise alone. Results are given for beam switching and for OTF mapping at several observing frequencies. Also given in Table 3 are the coefficients G_1 required to produce this amount of error if the gain fluctuations are entirely of the "$1/f$" type, $S_g(f) = G_1(1\,\mathrm{Hz}/f)$; the rms temperature change in time T if they are entirely due to a coefficient of .013/K, as reported for the BIMA IF amplifier/mixer/detector chain [16]; the rms temperature change in T if they are entirely due to a coefficient of .05/K, as reported for an SIS mixer at 3.8K [15]; and finally the rate of change $\dot G/G$ if only a steady gain drift occurs.

Lower $1/f$ noise and tighter temperature control are required for the beam switching mode than for the OTF mode because the 10 msec transition time between beam positions forces relatively long integrations in order to keep the observing efficiency high, so the thermal noise per integration is low. In OTF mode, there is no significant time lost between on-source integrations, so each can be short; additional integrating time is obtained by repeated scans, after obtaining off-source reference measurements. On the other hand, the longer interval between on-source and off-source measurements in OTF mode allows a larger gain difference to develop. With a $1/f$ gain spectrum, this tradeoff favors OTF. But if the gain spectrum is steeper, or if there is a steady drift, it favors beam switching.

Comparing the values of G_1 in Tables 1 and 3 shows that nearly all of the cryogenic amplifiers tested have intrinsic gain fluctuations that would produce radiometer errors larger than the thermal noise in the ALMA application, usually several times larger. The NRAO prototype 8–12 GHz IF preamplifiers for ALMA SIS mixer receivers use transistors that are not represented in Table 1 (the "Cryo-3" wafer from JPL for the input stage). By taking the median normalized value from Table 1, $G_{1,\mathrm{norm}} = 3.0\times10^{-9}\,\mu\mathrm{m}^2\mathrm{Hz}^{-1}$, and scaling to $N = 3$, $T = 4.0\,\mathrm{K}$, and $A = 20\,\mu\mathrm{m}^2$ (stage 1) and $15\,\mu\mathrm{m}^2$ (stages 2 and 3), as appropriate to the prototype amplifiers [12], we estimate $G_1 = 1.2\times10^{-9}\,\mathrm{Hz}^{-1}$, which would produce errors at or slightly below the thermal noise in ALMA. It should be emphasized that this is just a rough estimate, that large device-to-device variations are possible, and that the cryogenic preamplifier may not be the largest contributor to gain fluctuations. In observations where this intrinsic gain fluctuation is the dominant cause of error, an improvement might be obtained by re-adjusting the bias for higher drain current; this will reduce the gain fluctuations but increase the noise temperature.

For the room temperature components, where we assume that most gain fluctuion is extrinsic, great care is needed to achieve an overall temperature coefficient less than a few percent per K, especially considering the large total gain required. Even with such a low temperature coefficient, Table 3 shows that stability better than 10 mK is needed to keep the gain fluctuation error below the thermal noise. On the time scales of interest here, 0.5 sec or less, this might be possible.

For SIS mixers, it appears that temperature regulation at the 3 mK level is needed to achieve the same goal. This is especially difficult because the time interval is comparable to the cycle time of the Gifford-McMahon cryocoolers intended for ALMA. If the mean temperature is higher than 3.8K, as seems likely, then the data in [7] indicates that the temperature coefficient will be worse.

Limitations Due To Atmospheric Turbulence

The desire to keep the effects of gain fluctuations below those of the thermal noise follows from the assumption that other effects on radiometer accuracy, in particular atmospheric turbulence, will also be below the thermal noise. There is evidence for this from site surveys and atmospheric modeling, but direct measurements of the fluctuations in emission and absorption of the atmosphere over ALMA's frequency range are not available on the time scales and angular scales that are relavent to the beam-switched and OTF observing modes under consideration. Instead, we have observations at the Atacama site of the phase fluctuations at 11 GHz in a fixed direction at relatively short sampling period (1 sec) from the site testing interferometer. From these the fluctuations in column density of water vapor can be derived, and by assuming that this same water vapor is the dominant cause of mm-submm absorption it is possible to derive the fluctuations in that absorbtion.

This exercise was done [3] in the context of the Millimeter Array project, which was intended to have a maximum frequency of about 350 GHz and a bandwidth of about 2 GHz per polarization. The interferometric path length was converted to 230 GHz opacity by $\Delta w = 6.3\Delta l$ and $\Delta\tau = r(f)\,\Delta w$ where w is the column density of water vapor, l is the microwave path length, τ is the opacity at frequency f, and $r(f)$ is the opacity per unit density of water. The value $r(230\,\mathrm{GHz}) = .03\,\mathrm{mm}^{-1}$ was derived from an atmospheric model. For ALMA, we now need to consider that the larger bandwidth reduces the thermal noise floor, and that we will be observing at higher frequencies.

It was found in [3] that at 230 GHz the 50th percentile fluctuations in antenna temperature at 0.1 sec interval should be $\Delta T_a = 5.3\,\mathrm{mK}$ (0.16 Jy at 30 Jy/K), or $\Delta T_a/T_{\rm sys} = 5.4\times10^{-5}$ if $T_{\rm sys} = 100\,\mathrm{K}$; extrapolating to .05 sec interval gives about 2.6×10^{-5}, which is adequate to support the beam switching case considered in Table 3. Similarly, at 0.5 sec interval they found 27 mK (0.8 Jy) or 2.6×10^{-4}, adequate for the OTF case at 270 GHz in Table 3, but only just equal to the thermal noise.

To convert the results to other frequencies, the FTS measurements reported in [21] can be used. These give zenith absorption from 150 to 1500 GHz derived from tipping measurements of emission. They cover only a brief time period (34 hours) during most of which the weather conditions were reported to have been excellent. Fitting the individual spectra to an atmospheric model shows that 90% of the absorption is explained by water vapor alone at all frequencies except near narrow oxygen lines. The opacity at any frequency varied with time by about a factor of 9, and the tipping procedure limited the time resolution to $\sim$15 min, but excellent correlation was found among frequencies in the various windows. For example, the ratios of 675 GHz and 875 GHz opacities to 220 GHz opacity were found to be 21.7 ± 0.2 and 23.0 ± 0.3, respectively. Assuming that the fluctuation scale $r(f)$ varies in the same way, we obtain the results in Table 4 for various frequencies in the sub-mm windows.

Table 4: Atmospheric Emission Fluctuation vs. Frequency
50th percentile rms fluctuations derived from data in [3] and [21].

f_L	τ_f/τ_{220}	$r(f_L)$	$\bar\tau$	$T_{\rm sys}$	$\Delta T_a/T_{\rm sys}$	
GHz	[21]	mm^{-1}		K	at .05 sec	at 0.5 sec
220	1.00	0.03	.070	101	2.6×10^{-5}	2.6×10^{-4}
345	$3.62\pm.03$	0.11	0.26	190	7.3×10^{-5}	7.3×10^{-4}
410	$7.05\pm.08$	0.21	0.50	256	1.2×10^{-4}	1.2×10^{-3}
675	21.7 ± 0.2	0.65	1.52	455	1.2×10^{-4}	1.2×10^{-3}
875	23.0 ± 0.3	0.69	1.62	537	1.2×10^{-4}	1.2×10^{-3}

Table 4 uses the 50th percentile fluctuations in water vapor derived from the test interferometer [3], but it uses, at each frequency, an average opacity $\bar{\tau}$ corresponding to 2 air masses at the median conditions that occurred during the clear-weather FTS observations in [21], which is far lower than the 50th percentile in average opacity, but closer to the conditions under which observations will be done at these frequencies. Measurements at 220 GHz covering all of calendar year 2002 [22] indicate that these conditions occur at the 11th percentile. A proper analysis requires knowledge of the joint statistics of total water vapor and fluctuations in water vapor (turbulence), and the appropriate data is available in the form of simultaneous measurements of 220 GHz emission and of 11 GHz phase fluctuations, but it has not yet been examined in this way.[2] The total and the fluctuations total are not related deterministically, but there is a weak correlation [26]. At 220 GHz and below, where the total opacity is usually low, the statistics of total water vapor are less important and can be ignored.

The system temperatures in Table 4 are computed from $T_{\rm sys} = (250\,{\rm K})(1 - e^{-\bar{\tau}}) + 8hf_L/k$, where the first term is an estimate of the atmospheric emission and the second is an estimate of the receiver noise.

Comparing Tables 3 and 4, it seems that atmospheric emission fluctuations will be larger than the thermal noise at 345 GHz and above, for both beam switching and OTF mapping. At 410 GHz and above, the rms error will be at least 2 times worse for beam switching and 10 times worse for OTF mapping. Nevertheless, this does not allow the gain stability requirements to be relaxed because they were already less stringent at the higher frequencies. At 270 GHz and below, where the atmosphere is more transparent and hence its emission is more stable, the radiometric sensitivity of ALMA will be limited by gain fluctuations unless their magnitudes are below those suggested by the first two lines of Table 3. This assumes that ALMA's overall gain stability is similar at all bands, and this should be the case because the components believed to be most important to the gain stability are common or identical.

Calibration

So far, we have considered only the question of whether the *sensitivity* of wide-band continuum radiometry might be limited by gain fluctuations. In the planned observing modes, we found that only the gain variations on time scales less than 1 sec are important. A separate issue is the calibration of the telescope, which is mainly a matter of determining the absolute value of the overall gain g rather than just its fluctuations. For interferometry, knowledge of the complex gain is needed, while for radiometry knowledge of $|g|$ is enough.

Absolute calibration is expected to rely primarily on observations of known astronomical sources, involving integration times and time intervals much larger than 1 sec. It is possible to adopt a two-tiered strategy, where variations in gain are tracked over relatively short time intervals (a few seconds to minutes) using standards built into the telescope, and absolute gain is determined less often (many minutes) using celestial standards. The details of the process are beyond the scope of this report, and indeed the strategies most appropriate for the various modes of ALMA are still being debated. Clearly, though, the accuracy of calibration is limited by any variation in gain over the intervals between measurements against some standard. A calibration accuracy goal of 1% in power has been suggested [23], although it is usually assumed that this will be limited by unmeasured effects of the atmosphere rather than gain variations of the instrument. Interferometric phase calibration is likely to be far worse than this, with a goal of 10% (0.1 radian) [24]. (Phase stability will be the subject of a separate report.)

We take the interval between absolute astronomical calibrations to be no larger than 1000 sec. (Sometimes it may be possible to make the interval much shorter.) Then it is reasonable to adopt the requirement that $|g|^2$ not vary by more than 0.5% and that $\angle g$ not vary by more than 0.04 radian over this interval, since not all of the error can be allocated to gain changes. If the dominant cause of gain variation for such intervals is physical temperature, then the data in Table 2 imply that temperature stability over such time intervals should be better than 0.38 K for room temperature components and better than .02 to 0.1 K for SIS mixers.

[2] Such an analysis is underway, so more definitive results should soon be available. Meanwhile, the arguments given here can be considered a rough indication of what to expect.

Acknowledgements

The author thanks Marian Pospieszalski, Simon Radford, and Mark Holdaway for valuable discussions and for supplying copies of some difficult-to-find references.

REFERENCES

[1] R. Brown, ALMA Project Book, chapter 2, "Requirements and specifications." Section III.2 of version 4.0 (last reviewed version); or section 1.III.2 of version 5.5 (unchanged); 2000-Apr-25. http://www.alma.nrao.edu/projectbk/construction/archived/project_book20010801/construc

[2] W. J. Welch, "Total power observing with the ALMA antennas." ALMA Memo No. 454, March 2000 (as a report to the ALMA Scientific Advisory Committee; distributed as an ALMA Memo in April 2003).

[3] M. A. Holdaway, F. N. Owen, and D. T. Emerson, "Removal of Atmospheric Emission from Total Power Continuum Observations." ALMA Memo No. 137, September 1995.

[4] B. Butler and E. Pangole, ALMA system level requirements document, in preparation.

[5] S. Guilloteau and B. Butler, ALMA calibration plan, in preparation.

[6] E. Wollack and M. Pospieszalski, "Characteristics of broadband InP millimeter-wave amplifiers for radiometry." IEEE MTT-S Digest, 1998, pp 669–671.

[7] J. Kooi, G. Chattopadhyay, M. Thielman, and T. Phillips, "Noise stability of SIS receivers." *Int. J. of Infrared and Millimeter Waves*, vol 21, pp 680–716 (May 2000).

[8] B. Lazareff, "Stability of the IRAM 30m receivers." IRAM internal technical note, 28-Mar-2001.

[9] D. Allan, "Statistics of atomic frequency standards. *Proc. IEEE*, vol 54, pp 221–230 (Feb. 1966).

[10] J. Barnes et al., "Characterization of frequency stability." *IEEE Trans. Instr. & Meas.*, vol IM-20, pp 105–120 (May 1971).

[11] A. Miller et al., "The QMAP and MAT/TOCO experiments for measuring anisotropy in the cosmic microwave background." *Ap. J.*, submitted, 2003.

[12] M. Pospieszalski, private communication (April 2003).

[13] J. Gallego and I. Fernández, "Measurements of gain fluctuations in GaAs and InP cryogenic HEMT amplifiers." Centro Astronomico de Yebes, Spain, technical report 2000-1 (Feb. 2000).

[14] E. Wollack, "High-electron-mobility-transistor gain stability and its design implications for wide band millimeter wave receivers." *Rev. Sci. Instrum.* vol 66, pp 4305–4312 (Aug. 1995).

[15] R. Plambeck et al., "Interferometer phase correction from receiver total power measurements." National Radio Science Meeting (URSI), Boulder, CO, Jan. 1996.

[16] B. Frye et al., "Gain and phase stabilities of some components used in the BIMA array." MMA (ALMA) Memo No. 131, July 1995.

[17] A. Beryshev et al., "Influence of temperature variations on the stability of a submm wave receiver." 14th International Symposium on Space Terahertz Technology, Tucson AZ, April 2003.

[18] B. Lazareff, "Stability of IRAM-30m receivers." Technical note dated 28-Mar-2001 (unpublished).

[19] R. Plambeck, private communication to A. Perfetto, 26 March 2001.

[20] ALMA Project, "Subreflector position control." Project Book version 4.0, section 4.2.9, 2001-Feb-06. (See [1] for URL.)

[21] S. Matsushita et al., "FTS measurements of submillimeter-wave atmospheric opacity at Pampa la Bola II: Supra-Terahertz windows and model fitting." *Pub. Astron. Soc. Pacific*, vol 51, pp 603 ff (1999).

[22] S. Radford, data from 220 GHz tipping radiometer at Chajnantor for CY2002. http://www.tuc.nrao.edu/alma/site/Chajnantor/data.c.html

[23] ALMA Project, "Calibration Requirements." Project Book version 4.0, subsection of Chapter 2.2, 2001-Feb-06. (See [1] for URL.)

[24] ALMA Project, "Phase errors." Project Book version 4.0, subsection 7.0.6 of Local Oscillators chapter, 2001-Feb-05. (See [1] for URL.)

[25] N. Jarosik, "Measurements of the low-frequency-gain fluctuations of a 30-GHz high-electron-mobility-transistor cryogenic amplifier." *IEEE Trans. Microwave Thy. & Tech.*, vol 44, pp 193–197 (1996).

[26] S. Radford, "Site charaterization for mm/submm astronomy." In *Astronomical Site Evaluation in the Visible and Radio Range,* ASP Conference Series, vol 166 (2001).

APPENDIX A: Derivation of Radiometer Output Power Spectrum

Let $n(t)$ be bandlimited white Gaussian noise with bandwidth B, center frequency $f_0 >> B$, and noise temperature T_s, so that its (2-sided) power spectral density is $S_n(f) = kT_s/2$ for $f_0 - B/2 < |f| < f_0 + B/2$ and zero elsewhere. Using the radiometer model of Fig. 1,

$$v(t) = [g(t)\, n(t)]^2 \tag{A1}$$

where we have temporarily ignored the influence of the lowpass filter at the output. The autocorrelation function of $v(t)$ is then

$$\begin{aligned} R_v(\tau) &= \langle [g(t)n(t)g(t-\tau)n(t-\tau)]^2 \rangle \\ &= \langle [g(t)g(t-\tau)]^2 \rangle \langle [n(t)n(t-\tau)]^2 \rangle \end{aligned} \tag{A2}$$

where we have assmued that $g(t)$ and $n(t)$ are independent. The first factor can be written

$$\begin{aligned} \langle [g(t)g(t-\tau)]^2 \rangle &= \langle [g_0 + \delta g(t)]^2 \, [g_0 + \delta g(t-\tau)]^2 \rangle \\ &= G_0^2 + 2g_0^3 \, \langle \delta g(t-\tau) \rangle + g_0^2 \langle \delta g(t-\tau)^2 \rangle + 4g_0^2 \langle \delta g(t) \, \delta g(t-\tau) \rangle \\ &\quad + 2g_0 \langle \delta g(t) \, \delta g(t-\tau)^2 \rangle + \langle \delta g(t)^2 \, \delta g(t-\tau)^2 \rangle. \end{aligned} \tag{A3}$$

Since $\langle \delta g \rangle = 0$ by definition, and letting $\langle \delta g^2 \rangle = \sigma_g^2$ and $R_g(\tau) = \langle \delta g(t) \, \delta g(t-\tau) \rangle$, this simplifies to

$$\langle [g(t)g(t-\tau)]^2 \rangle = G_0^2 + G_0 \, \sigma_g^2 + 4G_0 \, R_g(\tau) + \sigma_g^4 + 2R_g(\tau)^2 \tag{A4}$$

where the last term of (A3) was expanded by using the theorem

$$\langle abcd \rangle = \langle ab \rangle \langle cd \rangle + \langle ac \rangle \langle bd \rangle + \langle ad \rangle \langle bc \rangle \tag{A5}$$

which applies to zero-mean, normally distributed random variables. Finally, applying the same theorem to the second factor of (A2) and dividing by $P_0^2 \, G_0^2$, we find after some rearrangement

$$\frac{R_v(\tau)}{P_0^2 \, G_0^2} = 1 + \frac{\sigma_g^2 (G_0 + \sigma_g^2}{G_0^2} + \frac{R_g(\tau)[2G_0 + R_g(\tau)]}{G_0^2} + \left\{ 2 + \frac{4R_g(\tau)[2G_0 + R_g(\tau)]}{G_0^2} + \frac{\sigma_g^2 (G_0 + \sigma_g^2)}{G_0^2} \right\} \frac{R_n(\tau)^2}{P_0^2}. \tag{A6}$$

Now assume that the gain fluctuations are small, so $G_0 >> \sigma_g^2 \geq R_g(\tau)$. Then by neglecting terms of order σ_g^4/G_0^2 or smaller, (A6) simplifies to

$$\frac{R_v(\tau)}{P_0^2 \, G_0^2} = 1 + \sigma_g^2/G_0 + 2R_g(\tau)/G_0 + [2 + \sigma_g^2/G_0 + 8R_g(\tau)/G_0] \frac{R_n(\tau)^2}{P_0^2}. \tag{A7}$$

As a final assumption, let the gain fluctuations be slow compared with $1/B$, so that $R_g(\tau) \approx R_g(0) = \sigma_g^2$ for all τ where $R_n(\tau)$ is signficant, giving

$$\frac{R_v(\tau)}{P_0^2 \, G_0^2} = 1 + \sigma_g^2/G_0 + 2R_g(\tau)/G_0 + (2 + 9\sigma_g^2/G_0) \frac{R_n(\tau)^2}{P_0^2}. \tag{A8}$$

The desired normalized power spectrum of $v(t)$ is the Fourier transform of (A8), or

$$\frac{S_v(f)}{V_0^2} = (1 + \sigma_g^2/G_0) \, \delta(f) + \frac{2S_g(f)}{G_0} + (2 + 9\sigma_g^2/G_0) \frac{S_n(f) * S_n(f)}{(kT_sB)^2} \tag{A9}$$

where $*$ denotes convolution and we have used the facts that $P_0^2 \, G_0^2 = V_0^2$ and $P_0 = kT_sB$. The power spectrum $S_n(f)$ was given at the beginning of this Appendix, and its self-convolution is just $B(kT_s)^2/2$ for $|f| << B$. We have so far ignored the low pass filter (LPF) in Fig. 1, but it can now be accounted for by dropping the components of $S_n(f) * S_n(f)$ that are near $2f_0$. Using these facts and making the further approximation of dropping the terms in σ_g^2/G_0 from (A9), again because of the assumption that the gain fluctuations are small, we get the result quoted at equation (1).